

Radiomics for intracerebral hemorrhage: are all small hematomas benign?

Chen-yi Zhan

Department of Radiology, The First Affiliated Hospital of Wenzhou Medical University, 325000 Wenzhou, China

Qian Chen

Department of Radiology, The First Affiliated Hospital of Wenzhou Medical University, 325000 Wenzhou, China

Ming-yue Zhang

Department of Radiology, The First Affiliated Hospital of Wenzhou Medical University, 325000 Wenzhou, China

Jin-jin Liu

Department of Radiology, The First Affiliated Hospital of Wenzhou Medical University, 325000 Wenzhou, China

Yi-lan Xiang

Department of Radiology, The First Affiliated Hospital of Wenzhou Medical University, 325000 Wenzhou, China

Jie Chen

Department of Radiology, The First Affiliated Hospital of Wenzhou Medical University, 325000 Wenzhou, China

Dong-qin Zhu

Department of Radiology, The First Affiliated Hospital of Wenzhou Medical University, 325000 Wenzhou, China

Chao Chen

Department of Radiology, The First Affiliated Hospital of Wenzhou Medical University, 325000 Wenzhou, China

Tian-yi Xia

Department of Radiology, The First Affiliated Hospital of Wenzhou Medical University, 325000 Wenzhou, China

Yunjun Yang (✉ yyjunjim@163.com)

Wenzhou Medical University First Affiliated Hospital

Research

Keywords: intracerebral hemorrhage, hematoma expansion, outcome, radiomics, computed tomography

Posted Date: May 28th, 2020

DOI: <https://doi.org/10.21203/rs.3.rs-31053/v1>

License:  This work is licensed under a Creative Commons Attribution 4.0 International License.

[Read Full License](#)

Version of Record: A version of this preprint was published at The British Journal of Radiology on March 1st, 2021. See the published version at <https://doi.org/10.1259/bjr.20201047>.

Abstract

Background: Radiomics is a valuable tool for predicting hematoma expansion (HE) but has not been used for small intracerebral hemorrhage (ICH). We hypothesized that not all small hematomas are benign and that radiomics could predict HE and short-term outcomes in small hematomas.

Methods: We analyzed 313 patients with small ICH who underwent baseline noncontrast CT within 6 h of symptom onset between September 2013 and February 2019. Small ICH was defined as baseline hematoma volume <10 mL. A radiomic score (R-score) was developed in a training (n=218) and validated in a test cohort (n=95). Poor outcome was defined as a Glasgow Outcome Scale score ≤ 3 . The relationship of the R-score with HE and outcomes was investigated using univariate and multivariate analyses. Predictive performance was assessed by the area under the receiver operating characteristic (ROC) curve (AUC).

Results: R-score was an independent predictor of HE in the training (odds ratio [OR]: 2.557; 95% CI, 1.455–4.492) and test cohorts (OR, 3.985; 95% CI, 1.051–14.453). In the 3–10 mL subgroup, but not in the <3 mL subgroup, the R-score was independently associated with HE (OR, 4.293; 95% CI, 2.095–8.796) and poor outcome (OR, 1.297; 95% CI, 1.004–1.674) after adjusting for confounders. The R-score achieved good discrimination ability for HE in the training and test cohorts and the 3–10 mL subgroup (AUCs 0.728, 0.717, and 0.740, respectively).

Conclusions: Radiomics provides an objective and effective approach for discriminating between benign and malignant course in patients with small ICH, particularly 3–10 mL hematomas.

Introduction

Intracerebral hemorrhage (ICH) is the most devastating subtype of stroke with high morbidity and mortality [1]. Baseline hematoma volume is an independent predictor of hematoma expansion (HE) and poor outcome in patients with ICH [2, 3]. Although patients with smaller hematomas are more likely to have a benign clinical course [4, 5], some studies reported that small hemorrhage in deep locations caused functional dependence or mortality, and the volume cutoff to predict poor outcome was less than the widely used of 30 mL [6–8]. In a prior study, small ICH was defined as benign or malignant, and patients with the latter experienced HE and had worse outcomes [5].

Several clinical trials have also enrolled many patients with small-volume ICH [9–11], but these trials failed to demonstrate a clinical benefit of the intervention. One possibility might be that small ICH is malignant in only a proportion of patients and those with benign small ICH have little opportunity to benefit from treatment. Therefore, it is important to improve patient selection and identify those with malignant small hematomas at high risk of expansion. Currently, there is no standard definition of small hematoma [4, 5, 12, 13]. As the average ICH volume in clinical trials is approximately 10 mL, we defined small hematomas as those with a baseline hematoma volume less than 10 mL.

Radiomics is an emerging approach that extracts high-throughput quantitative features from medical images and enables us to utilize the full potential of images [14, 15]. It has been widely used for the prediction of cancer and differentiation of benign and malignant tumors [16, 17]. Recently, radiomic analyses have been applied to ICH for the prediction of HE [18-20]. However, clinical risk factors known to be associated with HE were not taken into account in these studies. Moreover, to the best of our knowledge, no study has applied radiomics to predict HE or the short-term outcomes in patients with small hematomas.

Therefore, in this study, we hypothesized that not all small hematomas (< 10 mL) are benign and that radiomics could predict HE and the short-term outcomes in patients with small hematomas.

Materials And Methods

Study design and patient population

We retrospectively analyzed the records of patients aged >18 years who presented with primary ICH at our Neurological Emergency Room between September 2013 and February 2019. The inclusion criteria were as follows: (1) a baseline noncontrast computed tomography (NCCT) scan performed within 6 h after symptom onset; (2) a follow-up NCCT scan performed within 72 h after the initial CT scan; (3) and Glasgow Outcome Scale (GOS) score evaluated at discharge. The exclusion criteria were as follows: (1) secondary ICH (tumor, trauma, cerebral aneurysm, arteriovenous malformation, or hemorrhagic transformation from brain infarction); (2) primary intraventricular hemorrhage (IVH) or multiple cerebral hemorrhage; (3) surgical evacuation before the follow-up NCCT scan; (4) anticoagulant-associated ICH; and (5) CT images with severe motion artifacts.

Patients were randomly assigned to the training or test cohorts. HE was defined as a relative increase of 33% or an absolute increase of 6 mL of a hematoma from the baseline volume [21]. Poor outcome was defined as a GOS score ≤ 3 at discharge [22-24].

This study was approved by the Medical Ethics Committee of The First Affiliated Hospital of Wenzhou Medical University. The requirement for written informed consent was waived owing to the retrospective design of the study.

Image acquisition and segmentation

All patients were examined using a 64-slice spiral CT scanner (LightSpeedVCT64; GE Medical Systems, Milwaukee, WI, USA). The baseline and follow-up CT scans were performed using a standard clinical protocol with an axial technique, with slice thickness of 5 mm, tube voltage of 120 kV(p), and tube current of 80 mA.

Figure 1 illustrated the flow chart of the study. All images were analyzed by a radiologist (2-year experience) blinded to the patients' identity and clinical data. The contours of all intracerebral hematomas were drawn manually layer-by-layer. Fifty images were randomly chosen and were assessed

by another radiologist (5-year experience). The ventricular extension was not included. Three-dimensional segmentation of the region of interest (ROI) was performed using the ITK-SNAP software (version 3.8, www.itksnap.org) (Figure 2).

Clinical analysis

The essential clinical data, including age, sex, history of hypertension, diabetes mellitus, ischemic stroke, ICH, and Glasgow coma scale (GCS) scores, were recorded after admission. We also recorded the time from symptom onset to CT, location of the hematoma, presence of IVH, and hematoma volume after the initial NCCT scan. Two radiologists (2-year and 5-year experience) blinded to the patients' identity and clinical data interpreted the baseline NCCT images to assess the following features: (1) satellite sign; (2) black hole sign; (3) blend sign; and (4) Island sign. In case of discrepancy, the final decisions were reached by consensus.

Radiomic analysis

In our study, the set of radiomic features contained 396 descriptors from five groups: (1) first-order statistics of intensity (n=42), (2) shape (n=20), (3) gray-level co-occurrence matrix (n=144), (4) gray-level run length matrix (n=172), and (5) Haralick features (n=18). Feature extraction was performed using the Artificial Intelligence Kit version 3.0.0.R in the training cohort.

Least absolute shrinkage and selection operator (LASSO) logistic regression was used for feature selection to reduce redundancy. Ten-fold cross-validation was applied to choose the tuning parameter that determined the magnitude of penalization. Features with non-zero coefficients were selected to calculate the radiomic score (R-score) using the following formula:

$$\text{R-score} = \sum \beta_i X_i + \text{Intercept} \quad (i = 0, 1, 2, 3, \dots), \quad (1)$$

where X_i represents the i th selected radiomic features, and β_i is the respective coefficient determined by LASSO regression. We further validated the R-score in subgroups with volumes 3–10 mL and less than 3 mL. Receiver operating characteristic curve analysis was performed to assess the predictive performance with the associated classification measures. The Youden index (sensitivity + specificity-1) was used to select the cutoff value to determine the corresponding sensitivity and specificity. The reproducibility of the radiomic features was assessed using the interclass correlation coefficient (ICC), with an ICC greater than 0.75 indicating good interobserver agreement.

Evaluation of the clinical outcome at discharge

Univariate analysis was used for comparing the differences between patients with favorable (GOS score 4–5) and those with poor outcome (GOS score 1–3) in both subgroups (volumes of 3–10 mL and <3 mL). Multivariate logistic regression analysis with a backward step-wise selection was performed to determine the independent predictors.

Statistical analysis

For categorical variables, differences were calculated using the chi-square test or Fisher's exact test. Student's t-test or Mann-Whitney's U test was used for estimating the differences in continuous variables. Normally distributed continuous data were represented as mean \pm standard deviation, otherwise as median with interquartile range (IQR). Univariate analysis was used to compare the variables to discover the possible significant predictors for HE and poor outcome. Variables with $p < 0.05$ were included in the multivariate logistic regression analysis. The relative risk was estimated by odds ratios (ORs) with 95% confidence intervals (CIs) for each independent variable. All statistical analyses were performed with SPSS (version 22.0, IBM) and R statistical software (version 3.6.1, <https://www.r-project.org>). A two-sided p -value < 0.05 was considered statistically significant.

Results

Patients' characteristics

In total, 313 patients with ICH were included in the final analysis. There were 218 patients in the training cohort and 95 in the test cohort.

The baseline characteristics of the training and test cohorts are detailed in Table 1. The characteristics of the subgroups are presented in Tables S1 and S2. The incidence of HE was 13.8% (30 of 218) in the training cohort and 14.7% (14 of 95) in the test cohort. No significant difference was found between the two cohorts (all $p > 0.05$). In the subgroup analysis, HE was observed in 28 patients (11.2%) of the 3–10 mL subgroup and in 16 patients (25.8%) of the < 3 mL subgroup.

Development and validation of the R-score

After evaluating the differentiating ability of the radiomic features in the univariate analysis, 58 features with p -values < 0.05 were selected. These features were reduced to three potential predictors (kurtosis, HaralickCorrelation_AllDirection_offset1_SD, ShortRunHighGreyLevelEmphasis_AllDirection_offset4_SD) that had non-zero coefficients in the LASSO logistic regression model in the training cohort (Figure 3).

The R-score was then calculated using the following formula:

$$\text{R-score} = -2.180 - 0.299 \times \text{kurtosis} - 0.858 \times \text{HaralickCorrelation_AllDirection_offset1_SD} - 0.272 \times \text{ShortRunHighGreyLevelEmphasis_AllDirection_offset4_SD} \quad (2)$$

The calculated R-scores are summarized in Table 1. There were significant differences between the HE and non-HE (NHE) groups in the training and test cohorts, and the 3–10 mL subgroup (all $p < 0.001$; Tables 1, S1).

Table 1. Patients' baseline characteristics.

	Training cohort (n=218)			Test cohort (n=95)			P*
	HE (n=30)	NHE (n=188)	P value	HE (n=14)	NHE (n=81)	P value	
Age, y, mean(SD)	64.0(9.1).	62.6(12.0)	0.541	56.6(8.6)	63.1±11.9	0.022	0.657
Male	22(73.3)	106(56.4)	0.080	8(57.1)	46(56.8)	0.98	0.757
Medical history							
Arterial hypertension	26(86.7)	159(85)	1	11(78.6)	69(88.5)	0.384	0.695
Diabetes mellitus	6(20)	31(16.6)	0.644	3(21.4)	15(19.2)	1	0.597
ICH	1(3.3)	8(4.3)	1	2(14.3)	3(3.8)	0.165	0.765
Ischemic stroke	3(10)	10(5.3)	0.397	0	6(7.7)	0.586	0.859
IVH	4(13.3)	71(37.8)	0.009	3(21.4)	29(35.8)	0.37	0.902
Black hole sign	5(16.7)	10(5.3)	0.039	4(28.6)	2(2.5)	0.004	0.854
Blend sign	3(10)	5(2.7)	0.082	3(21.4)	3(3.7)	0.04	0.372
Island sign	2(6.7)	6(3.2)	0.303	0	3(3.7)	1	1
Satellite sign	9(30)	29 (15.4)	0.051	2(14.3)	16(19.8)	1	0.748
Location			0.851			0.084	0.279
Deep	25(83.3)	154(81.9)		8(57.1)	65(80.2)		
Other	55(16.7)	34(18.1)		6(42.9)	16(19.8)		
Hematoma volume, mL, mean(SD)	5.3 (3.0)	5.7 (2.6)	0.431	5.8(3.6)	6.2(2.5)	0.637	0.204
Time from onset to CT, h, mean(SD)	2.6(1.4)	3.1(1.5)	0.073	2.2 (1.3)	3.2(1.5)	0.02	0.853
Admission GCS score, median (IQR)	14 (10.5–15)	15 (14–15)	0.066	15(11–15)	15 (12–15)	0.928	0.156
R-score, median (IQR)	-1.257 (-2.055–-0.977)	-2.088 (-2.970–-1.077)	<0.001	-1.461 (-1.810–-1.230)	-2.097 (-2.824–-1.388)	<0.001	1
Poor outcome	23(76.7)	87(46.3)	0.002	10(71.4)	48(59.3)	0.389	0.084

All values are presented as count (%) unless otherwise specified. CT, computed tomography; HE, hematoma expansion; NHE, non-hematoma expansion; GCS, Glasgow coma scale; ICH, intracerebral hemorrhage; IVH, intraventricular hemorrhage; R-score, radiomic score; SD, standard deviation; IQR, interquartile range. * Indicates comparison between the training and test cohorts.

Association between the R-score and HE

In the training cohort, IVH, black hole sign, and the R-score significantly differed (all $p < 0.05$) between the HE and NHE groups (Table 1). Multivariate logistic regression analysis indicated the R-score (OR, 2.557; 95% CI, 1.455–4.492; $p = 0.001$) as an independent predictor of HE (Table 2).

In the test cohort, age, black hole sign, blend sign, time from symptom onset to CT, and the R-score significantly differed between the HE and NHE groups (Table 1). The R-score (OR, 3.898; 95% CI, 1.051–14.453; $p = 0.042$) was also independently associated with HE (Table 2).

Table 2. Multivariate analysis for hematoma expansion in the training and test cohorts.

Variables	Training cohort		Test cohort	
	OR (95% CI)	P Value	OR (95% CI)	P Value
IVH	0.292 (0.096–0.890)	0.030	NA	NA
R-score	2.557 (1.455–4.492)	0.001	3.898(1.051–14.453)	0.042
Black hole sign	2.710 (0.759–9.677)	0.125	10.326(1.330–80.186)	0.026
Blend sign	NA	NA	3.985 (0.332–47.897)	0.276
Age	NA	NA	0.930(0.869–0.996)	0.037
Time from onset to CT	NA	NA	0.557 (0.307–1.011)	0.054

OR, odds ratio; CI, confidence interval; CT, computed tomography; R-score, radiomic score; IVH, intraventricular hemorrhage; NA, not available.

In the 3–10 mL subgroup, patients with HE had higher rates of black hole sign and blend sign, larger hematoma volumes, lower GCS scores, and higher R-scores (Table S1). The R-score was independently associated with HE (OR, 4.293; 95% CI, 2.095–8.796; $p < 0.001$) after adjusting for confounders (Table 3). In the <3 mL subgroup, univariate analysis showed that there was no significant difference in the R-score between the HE and NHE groups (Table S2).

Table 3. Multivariate analysis for hematoma expansion and poor outcome in the 3–10 ml subgroup.

Variables	Hematoma expansion		Poor outcome	
	OR (95% CI)	P Value	OR (95% CI)	P Value
Blend sign	4.748(1.114–20.246)	0.035	NA	NA
Hematoma volume	1.385(1.088–1.762)	0.008	NA	NA
Admission GCS score	0.869(0.765–0.987)	0.031	0.737(0.643–0.844)	<0.001
R-score	4.293(2.095–8.796)	<0.001	1.297(1.004–1.674)	0.046
Location, deep	NA	NA	5.167(2.104–12.689)	<0.001
Black hole sign	2.311 (0.666–8.021)	0.187	3.460 (0.724–16.546)	0.120
Island sign	NA	NA	3.641 (0.758–17.487)	0.106

OR, odds ratio; CI, confidence interval; GCS, Glasgow coma scale; R-score, radiomic score; NA, not available.

In the training cohort, the area under the curve (AUC) value of the R-score was 0.728 (95% CI, 0.631–0.826) (Table S3, Figure 4). In the test cohort, the R-score showed an AUC value of 0.716 (95% CI, 0.596–0.836). The AUC value was 0.740 (95% CI, 0.659–0.820) in the 3–10 mL subgroup. Furthermore, the optimal cutoff value for the R-score was -1.430 in the training cohort according to the Youden index. The interobserver agreement on the radiomic features reached a mean ICC of 0.89.

Association between the R-score and short-term poor outcomes

Of the 313 patients with small ICH, 168(53.7%) had poor outcomes at discharge. In the two subgroups, 143 (57%) of the 251 patients in the 3–10 mL subgroup and 25(40.3%) of the 62 patients in the <3 ml subgroup had poor outcomes. The rate of poor outcome was significantly lower in the 3–10 mL subgroup (40.3% versus 57%; $p = 0.019$).

In the 3–10 mL subgroup, patients with poor outcomes had a higher frequency of the black hole sign (9.8% versus 2.8%, $p = 0.029$) and island sign (6.3% versus 0.9%, $p = 0.047$), lower admission GCS scores (median, 14 [IQR, 11–15] versus 15 [IQR, 15–15]; $p < 0.001$), higher R-scores (median, -1.968 [IQR, -2.749–-1.288] versus -2.382 [-3.257– -1.427]; $p = 0.024$), and a higher rate of deep ICH(90.0% versus 75.9%, $p = 0.001$) (Table S1). The multivariate logistic regression analysis indicated that deep location (OR, 5.167; 95% CI, 2.104–12.689; $p < 0.001$), the GCS score (OR, 0.737; 95% CI, 0.643–0.844; $p < 0.001$), and the R-score (OR, 1.297; 95% CI, 1.004–1.674; $p = 0.046$) were independent predictors of poor outcomes (Table 3). In the <3 ml subgroup, the univariate analysis showed no significant difference in the R-score between patients with poor and those with favorable outcome (Table S2).

Discussion

In this retrospective study, we established an R-score to predict HE in small hematomas (<10 mL). We additionally explored the association between the R-score and short-term poor outcomes in subgroups with hematoma volumes of 3–10 mL and less than 3 mL. Our results indicated that small hematomas could exhibit a malignant course and that the R-score based on NCCT was strongly associated with HE. We also found that the R-score could independently predict poor outcomes in small hematomas with a volume of 3–10 mL, but not in very small hematomas with a volume of less than 3 mL.

To date, most trial inclusion criteria and clinical grading scales have used a cutoff of 30 mL to identify patients likely to have a malignant clinical course with a high expansion rate and a poor outcome[3, 24, 25]. However, hematomas less than 10 mL could account for approximately one-third to one-half of all patients with ICH [5, 13, 26] and their destructive effects should not be underestimated. One study demonstrated that baseline hematoma size categories of <10 mL had the same ability to predict outcome regardless of the HE definition[21]. Ironside et al. modified the original ICH score and the volume cutoff was less than 10 mL in the deep and brainstem location[8]. Therefore, it is meaningful to discriminate hematomas with a benign clinical course from those with a malignant course so the effects of interventions could be improved. Our results showed that very small hematomas (<3 mL) had a higher rate of HE compared to those with a volume of 3–10 mL, but with a more benign outcome. We further confirmed the findings of other studies that demonstrated very small hematomas were likely to have benign outcomes[12, 13]. This may indicate that the very small growth in very small hematomas is insufficient to translate into functional deterioration and the benefits of anti-expansion therapy in those patients may be outweighed by the potential of harm.

Recently, several radiographic features have been used to predict HE and poor outcome, including the black hole sign, blend sign, satellite sign, and CT angiography (CTA) spot sign[27, 28]. Li et al. reported that patients with benign ICH who had none of these signs would not experience HE[5]. Their definition was complicated for inexperienced radiologists and clinical physicians to make accurate and fast identification. Our R-score could objectively identify patients with HE whose NCCT signs were negative. In the Antihypertensive Treatment of Acute Cerebral Hemorrhage II (ATACH-II) trial, there was no evidence that patients with ICH with CTA spot sign or NCCT signs would benefit from intensive blood pressure reduction[29, 30]. It is uncertain whether these signs were inadequate to identify the patients most likely to benefit due to their subjective judgment and somewhat overlapped definition. In addition, the CTA spot sign is unsuited in the emergency room, particularly for patients with ICH with kidney insufficiency and contrast agent allergies, because it is time-consuming and requires a contrast injection. Therefore, quantitative NCCT predictors have been sought to identify subtle changes beyond visual assessment.

Radiomics was initially proved to be useful in tumor assessment due to its ability to quantify the heterogeneity of the ROI and was then applied to ICH[31]. Shen et al. demonstrated that by using the Laplacian of the Gaussian bandpass filter, NCCT textures could discriminate between HE and NHE[20]. However, only histogram-based features were analyzed in 108 patients with ICH, which limited the comprehensive assessment of hematoma heterogeneity compared with that achievable with radiomic signatures. Subsequently, Ma et al. reported that a five-feature-based R-score could independently

evaluate the risk for HE with an accuracy of 0.852[19]. Another study also showed that the radiomic model had an accuracy of 0.726 in predicting HE and the AUC value was 0.729[18]. In accordance with these studies, the R-score in our study showed a good capability of predicting HE (with AUCs of 0.716–0.740), except in very small hematomas. This may further prove that very small hematomas are homogenous and would have a benign course. Recently, Xie et al. compared the NCCT-based radiomic model with the conventional radiological model in the prediction of HE[32]. Their analysis revealed that the radiomic model was a reliable and objective method for HE prediction and outperformed the radiological model. Our results also confirmed that the R-score was independently associated with HE after adjusting for confounders. Moreover, we found that in the 3–10 mL baseline hematoma volume category, the R-score was not only associated with HE but could independently predict poor outcomes at discharge. It should be more beneficial if the predictor is not only associated with HE but also related to poor outcomes. Our findings might have clinical implications for future clinical trials or practices, improving the ability to stratify the risk for HE or poor outcomes in patients with small hematomas. Because of the high density of hematomas relative to the surrounding edema or brain parenchyma, semi-automatic or automatic segmentation of hematomas may be applicable in the future, making it more convenient to apply radiomics.

There are some limitations in our study. First, it was a single-center retrospective study with a relatively small sample size. The small dataset may influence the performance of the R-score in the training cohort and reduce the reliability of the verification in the test cohort. Further multi-center studies with larger samples are needed to support our findings. Second, the finding cannot be applied to all types of ICH due to the exclusion of patients with secondary ICH and anticoagulant treatment. Finally, the GOS score at discharge was the only prognostic indicator. Whether long-term neurological deterioration or mortality is associated with the R-score should be further investigated.

Conclusions

The R-score could provide a noninvasive, objective, and reproducible method for discriminating between benign and malignant clinical course in patients with small ICH, particularly hematomas with a volume of 3–10 mL. Radiomics can be used as a supplement to conventional medical imaging, improving clinical decision-making and facilitating personalized treatment in ICH.

Declarations

Ethics approval and consent to participate

This study was approved by the Medical Ethics Committee of The First Affiliated Hospital of Wenzhou Medical University. The requirement for written informed consent was waived owing to the retrospective design of the study.

Consent for publication

All authors have read and approved the content and agree to submit for consideration for publication in the journal

Availability of data and materials

The datasets used and/or analysed during the current study are available from the corresponding author on reasonable request.

Competing interests

The authors declare that they have no competing interests.

Funding

The Science and Technology Planning Projects of Wenzhou (grant no. Y20180112), the Health Foundation for Creative Talents in Zhejiang Province, China (grant no.: 2016), and the Project Foundation for the College Young and Middle-aged Academic Leader of Zhejiang Province, China (grant no.: 2017).

Author Contributions

All authors have had access to the data and all drafts of the manuscript. Specific contributions are as follows: study design: C-Y.Z., Y-J.Y., Q.C.; data collection: C-Y.Z., Q.C., M-Y.Z., Y-L.X., J.C., D-Q.Z., C.C., T-Y.X.; data management and analysis: C-Y.Z., Q.C., M-Y.Z., J-J.L.; manuscript drafting: C-Y.Z., Q.C.; manuscript review: all. All authors read and approved the final manuscript.

Acknowledgments

We would like to thank Editage (www.editage.cn) for English language editing.

References

1. van Asch CJJ, Luitse MJA, Rinkel GJE, van der Tweel I, Algra A, Klijn CJM: Incidence, case fatality, and functional outcome of intracerebral haemorrhage over time, according to age, sex, and ethnic origin: a systematic review and meta-analysis. *The Lancet Neurology* 2010, 9(2):167-176.
2. R A-SS, J F, RJ L, PD L, TWK B, AM A, JN G, SA M, T S, X W *et al*: Absolute risk and predictors of the growth of acute spontaneous intracerebral haemorrhage: a systematic review and meta-analysis of individual patient data. *The Lancet Neurology* 2018, 17(10):885-894.
3. JC H, DC B, L B, GT M, SC J: The ICH score: a simple, reliable grading scale for intracerebral hemorrhage. *Stroke* 2001, 32(4):891-897.
4. Barras CD, Tress BM, Christensen S, MacGregor L, Collins M, Desmond PM, Skolnick BE, Mayer SA, Broderick JP, Diringner MN *et al*: Density and shape as CT predictors of intracerebral hemorrhage growth. *Stroke* 2009, 40(4):1325-1331.

5. Li Q, Yang WS, Shen YQ, Xie XF, Li R, Deng L, Yang TT, Lv FJ, Lv FR, Wu GF *et al*: Benign Intracerebral Hemorrhage: A Population at Low Risk for Hematoma Growth and Poor Outcome. *J Am Heart Assoc* 2019, 8(8):e011892.
6. AC L, KN S, M C, C A, BB W, A V, J R, C L, CJ M, D W *et al*: Identification and Validation of Hematoma Volume Cutoffs in Spontaneous, Supratentorial Deep Intracerebral Hemorrhage. *Stroke* 2019, 50(8):2044-2049.
7. K N, SL K, TB S: Optimal Hematoma Volume Cut Points to Predict Functional Outcome After Basal Ganglia and Thalamic Hemorrhages. *Frontiers in neurology* 2018, 9:291.
8. Ironside N, Chen CJ, Dreyer V, Christophe B, Buell TJ, Connolly ES: Location-specific differences in hematoma volume predict outcomes in patients with spontaneous intracerebral hemorrhage. *Int J Stroke* 2020, 15(1):90-102.
9. AI Q, YY P, WG B, DF H, CY H, RL M, CS M, R S, T S, JI S *et al*: Intensive Blood-Pressure Lowering in Patients with Acute Cerebral Hemorrhage. *The New England journal of medicine* 2016, 375(11):1033-1043.
10. N S, K F, JP A, R A-SS, D B, M B, H C, A C, R C, A C *et al*: Tranexamic acid for hyperacute primary IntraCerebral Haemorrhage (TICH-2): an international randomised, placebo-controlled, phase 3 superiority trial. *Lancet (London, England)* 2018, 391(10135):2107-2115.
11. C D, Y H, H A, J C, SM D, EL H, J W, MW P, G L, CS A: Hematoma growth and outcomes in intracerebral hemorrhage: the INTERACT1 study. *Neurology* 2012, 79(4):314-319.
12. D D, EE S, ML F, M A, P L, AM D: Small intracerebral haemorrhages are associated with less haematoma expansion and better outcomes. *International journal of stroke : official journal of the International Stroke Society* 2011, 6(3):201-206.
13. D D, V Y, RI A, D R-L, CA M, Y S, I D, A C, JM B, C L *et al*: Small intracerebral hemorrhages have a low spot sign prevalence and are less likely to expand. *International journal of stroke : official journal of the International Stroke Society* 2016, 11(2):191-197.
14. RJ G, PE K, H H: Radiomics: Images Are More than Pictures, They Are Data. *Radiology* 2016, 278(2):563-577.
15. Mayerhoefer ME, Materka A, Langs G, Haggstrom I, Szczypinski P, Gibbs P, Cook G: Introduction to Radiomics. *J Nucl Med* 2020, 61(4):488-495.
16. T C, Z N, L X, X F, S H, HR R, W X, X Z, Y H, H L *et al*: Radiomics nomogram for predicting the malignant potential of gastrointestinal stromal tumours preoperatively. *European radiology* 2019, 29(3):1074-1082.
17. Nie P, Yang G, Wang Z, Yan L, Miao W, Hao D, Wu J, Zhao Y, Gong A, Cui J *et al*: A CT-based radiomics nomogram for differentiation of renal angiomyolipoma without visible fat from homogeneous clear cell renal cell carcinoma. *European radiology* 2020, 30(2):1274-1284.
18. H L, Y X, X W, F C, J S, X J: Radiomics features on non-contrast computed tomography predict early enlargement of spontaneous intracerebral hemorrhage. *Clinical neurology and neurosurgery* 2019, 185:105491.

19. C M, Y Z, T N, J W, G G, J L, S L, F L, P Y, K W *et al*: Radiomics for predicting hematoma expansion in patients with hypertensive intraparenchymal hematomas. *European journal of radiology* 2019, 115:10-15.
20. Q S, Y S, Z H, W C, B Y, J H, Y H, W X, Z F: Quantitative parameters of CT texture analysis as potential markers for early prediction of spontaneous intracranial hemorrhage enlargement. *European radiology* 2018, 28(10):4389-4396.
21. D D, AM D, ML F, M A, PL L, EE S: Defining hematoma expansion in intracerebral hemorrhage: relationship with patient outcomes. *Neurology* 2011, 76(14):1238-1244.
22. JY J, W X, WP L, GY G, YH B, YM L, QZ L: Effect of long-term mild hypothermia or short-term mild hypothermia on outcome of patients with severe traumatic brain injury. *Journal of cerebral blood flow and metabolism : official journal of the International Society of Cerebral Blood Flow and Metabolism* 2006, 26(6):771-776.
23. M Z, T B, L D, R K, L S, J T, H VL, HS Y, T T, A P *et al*: Early surgical treatment for supratentorial intracerebral hemorrhage: a randomized feasibility study. *Stroke* 1999, 30(9):1833-1839.
24. Rost NS, Smith EE, Chang Y, Snider RW, Chanderraj R, Schwab K, FitzMaurice E, Wendell L, Goldstein JN, Greenberg SM *et al*: Prediction of functional outcome in patients with primary intracerebral hemorrhage: the FUNC score. *Stroke* 2008, 39(8):2304-2309.
25. JP B, TG B, JE D, T T, G H: Volume of intracerebral hemorrhage. A powerful and easy-to-use predictor of 30-day mortality. *Stroke* 1993, 24(7):987-993.
26. Wang X, Arima H, Al-Shahi Salman R, Woodward M, Heeley E, Stapf C, Lavados PM, Robinson T, Huang Y, Wang J *et al*: Clinical prediction algorithm (BRAIN) to determine risk of hematoma growth in acute intracerebral hemorrhage. *Stroke* 2015, 46(2):376-381.
27. Wada R, Aviv RI, Fox AJ, Sahlas DJ, Gladstone DJ, Tomlinson G, Symons SP: CT angiography "spot sign" predicts hematoma expansion in acute intracerebral hemorrhage. *Stroke* 2007, 38(4):1257-1262.
28. G B, A M, A C, D D, JN G: Noncontrast Computed Tomography Markers of Intracerebral Hemorrhage Expansion. *Stroke* 2017, 48(4):1120-1125.
29. A M, G B, JM R, HB B, MJ J, A V, K S, MR A, C C, SM G *et al*: Blood pressure reduction and noncontrast CT markers of intracerebral hemorrhage expansion. *Neurology* 2017, 89(6):548-554.
30. A M, HB B, JM R, MJ J, A V, K S, MR A, C C, SM G, RH M *et al*: Intensive Blood Pressure Reduction and Spot Sign in Intracerebral Hemorrhage: A Secondary Analysis of a Randomized Clinical Trial. *JAMA neurology* 2017, 74(8):950-960.
31. Z L, S W, D D, J W, C F, X Z, K S, L L, B L, M W *et al*: The Applications of Radiomics in Precision Diagnosis and Treatment of Oncology: Opportunities and Challenges. *Theranostics* 2019, 9(5):1303-1322.
32. Xie H, Ma S, Wang X, Zhang X: Noncontrast computer tomography-based radiomics model for predicting intracerebral hemorrhage expansion: preliminary findings and comparison with conventional radiological model. *European radiology* 2020, 30(1):87-98.

Figures

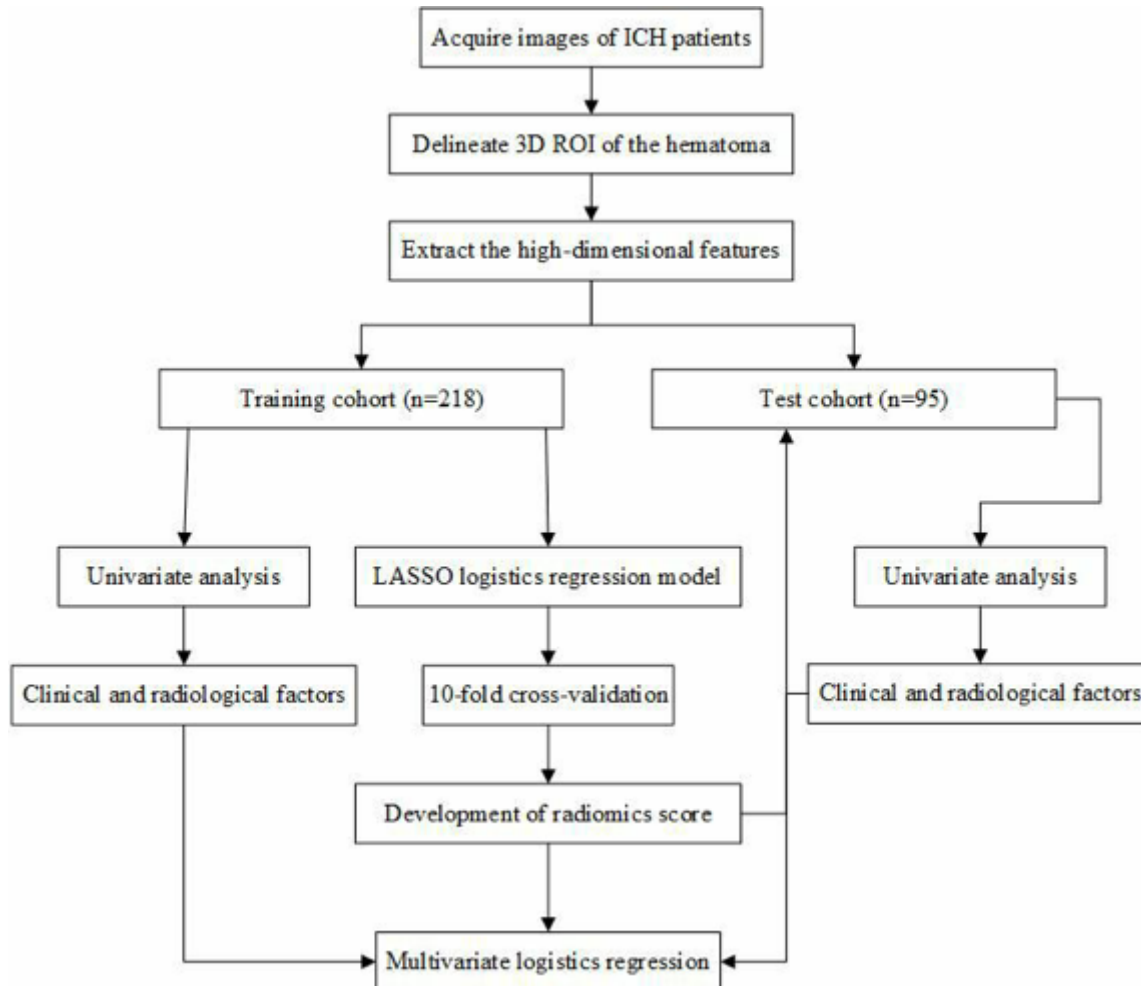


Figure 1

Flow chart of the study.

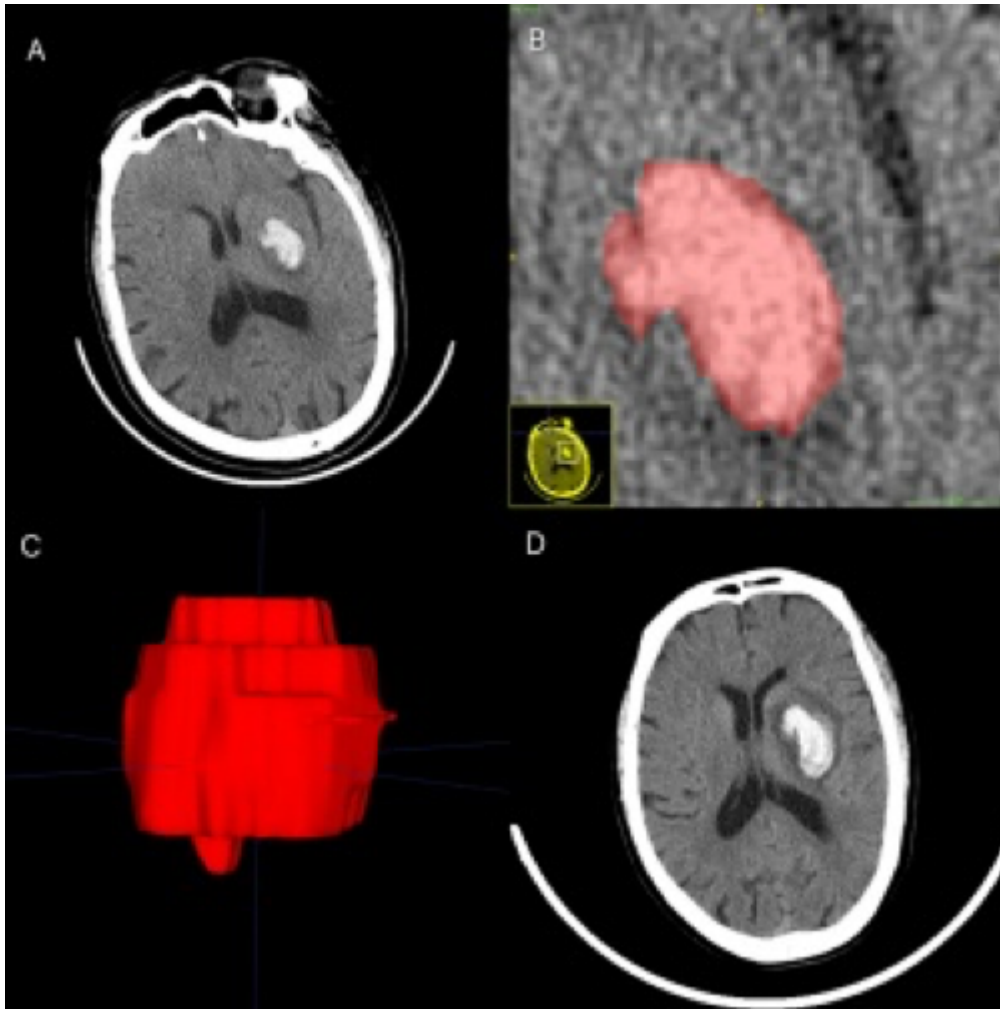


Figure 2

Manual three-dimensional (3D) segmentation of the hematoma. A) The patient's baseline computed tomography (CT) showed a small hematoma in the left basal ganglia (58 years, male, baseline volume = 7.41 mL, radiomic score = -1.145). B) Delineation of the lesion using the ITK-SNAP software. C) Generation of a 3D region of interest. D) Detection of hematoma expansion on follow-up CT (volume = 16.92 mL, Glasgow outcome scale score = 3).

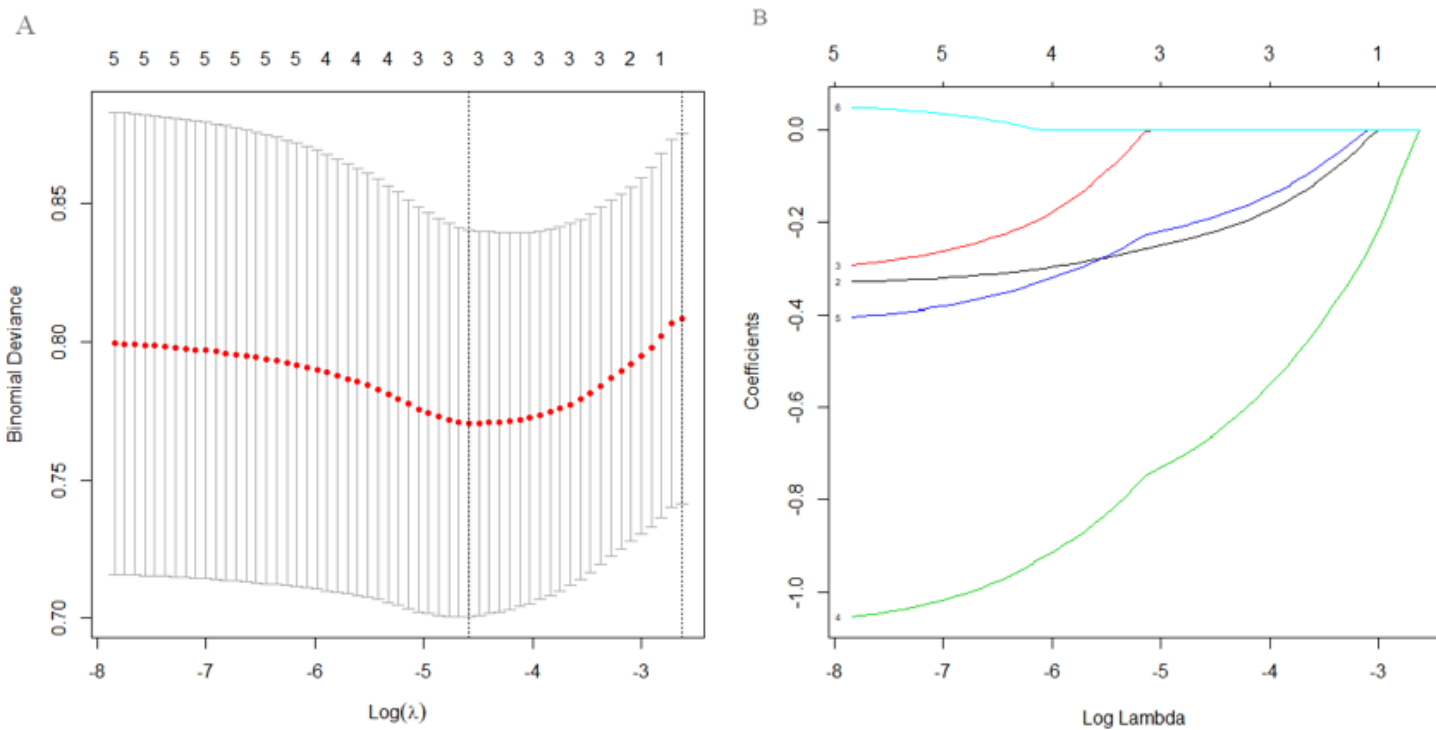


Figure 3

Radiomic feature selection using the least absolute shrinkage and selection operator (LASSO) regression model. We used 10-fold cross-validation to tune parameter (λ) selection in the LASSO model. A) AUC was plotted versus $\text{log}(\lambda)$. Three features with non-zero coefficients were selected using the minimum criteria. B) LASSO coefficient profiles of the features. Each colored line represents the coefficient of each feature.

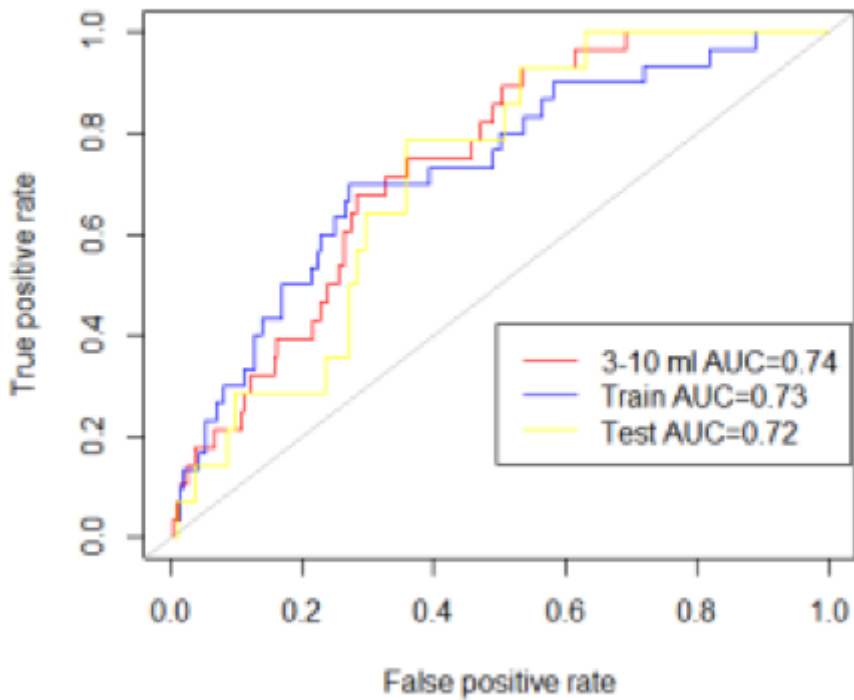


Figure 4

The receiver operating characteristic curves for the radiomic score in the three cohorts. AUC, area under the curve.

Supplementary Files

This is a list of supplementary files associated with this preprint. Click to download.

- [Supplementarymaterial.docx](#)